# Synthesis of a Room Temperature Stable $12CaO \cdot 7Al_2O_3$ Electride from the Melt and Its Application as an Electron Field Emitter

Sung Wng Kim,* Yoshitake Toda, Katsuro Hayashi, Masahiro Hirano, and Hideo Hosono

*Frontier Collaborative Research Center, Tokyo Institute of Technology, 4259 Nagatsuta, Midori-ku, Yokohama 226-8503, Japan*

*Received October 27, 2005. Revised Manuscript Received February 10, 2006*

A room temperature (RT) stable electride was realized by thermally annealing an insulating $12CaO \cdot 7Al_2O_3$ (C12A7) single crystal in a calcium metal vapor. Here we report a simple and direct method for synthesizing polycrystalline C12A7 electride (C12A7:$e^-$); the solidification of a "melt" in a reducing atmosphere and the crystallization of a "glass" with an oxygen-deficient composition in a vacuum. The carbon-related anion ($C_2^{2-}$) presumably serves as the template for the formation of the C12A7 phase in the solidification process and may be spontaneously released from the lattice during the cooling process, leaving mobile electrons in the lattice. Also the $C_2^{2-}$ ions accommodated in the glass may play a significant role in the formation of C12A7:$e^-$ during the crystallization. The polycrystalline C12A7:$e^-$ exhibits an electrical conductivity up to 5 $S \cdot cm^{-1}$ at 300 K, which corresponds to an electron concentration of $\sim 3 \times 10^{19}$ $cm^{-3}$ and a nearly equal mobility of $\sim 0.1$ $cm^2 \cdot V^{-1} \cdot s^{-1}$ to that of the single crystalline C12A7:$e^-$. A large current density of $\sim 12$ $\mu A \cdot cm^{-2}$ is obtained in the electron field emission from a flat surface of the polycrystalline C12A7:$e^-$ with a work function of $\sim 0.6$ eV for an applied electric field of $2.4 \times 10^5$ $V \cdot cm^{-1}$. These simple synthetic methods make it possible to produce efficiently the electride in large volume, which will facilitate the C12A7:$e^-$ research, paving a way for various applications including cold electron emission.

## Introduction

Electrides[1] in which an electron acts as an anion are exotic materials, but they are promising for various applications as well, such as reducing agents, cold-cathode electron field emitters, thermionic power generators, and refrigeration devices.[2−4] Most of the electrides fabricated to date are composed of organic materials and they are, unfortunately, unstable at room temperature (RT), degrading upon exposure to air or moisture except for the recently found $Na^+$(TriPip222)($e^-$).[5] These instabilities have restricted the realization of practical applications of the organic electrides.[6−7] Matsuishi et al. overcame these drawbacks of the organic electrides by synthesizing a RT stable inorganic $12CaO \cdot 7Al_2O_3$ electride (C12A7:$e^-$) by replacing the extraframework oxide ions in C12A7 with electrons.[8]

The C12A7[9−13] refractory oxide has a unique crystal structure. The unit cell with a stoichiometric composition is composed of a positively charged $[Ca_{24}Al_{28}O_{64}]^{4+}$ lattice framework that contains 12 sub-nanometer-size cages with an inner free space of $\sim 0.4$ nm in diameter. Thus, each cage has a mean effective charge of $+1/3$ (+4 charges/12 cages) and it is connected with a neighbor cage by sharing a Ca−O−Al−O−Al−O 6-atom ring. To compensate for the positive charge of the lattice framework, two $O^{2-}$ ions (extraframework oxide ions) are accommodated in a unit cell, distributing randomly on the 12 cages. These oxide ions can be replaced by various monovalent anions such as halogen anions ($F^-$, $Cl^-$),[9−12] hydroxide ions ($OH^-$),[9−12] superoxide radicals ($O_2^-$),[13] oxygen anion radicals ($O^-$),[14,15] and hydride ions ($H^-$).[16] Furthermore, they are almost exclusively substituted by electrons ($e^-$).[8]

The substitution procedure of the extraframework oxide ions with electrons is to thermally anneal a C12A7 single crystal in a calcium metal vapor. The strong reduction treatment selectively extracts the extraframework oxide ions

* To whom correspondence should be addressed. E-mail: sw-kim@lucid.msl.titech.ac.jp. Phone: +81-45-924-5127. Fax: +81-45-924-5134.

(1) Dye, J. L. *Inorg. Chem.* **1997**, *36*, 3816−3826.
(2) Toda, Y.; Matuishi, S.; Hayashi, K.; Ueda, K.; Kamiya, T.; Hirano, M.; Hosono, H. *Adv. Mater.* **2004**, *16*, 685−689.
(3) Huang, R. H.; Dye, J. L. *Chem. Phys. Lett.* **1990**, *166*, 133−136.
(4) Petkov, V.; Billinge, S. J. L.; Vogt, T.; Ichimura, A. S.; Dye, J. L. *Phys. Rev. Lett.* **2002**, *89*, 75502.
(5) Redko, M. Y.; Jackson. J. E.; Huang, R. H.; D. L.; Dye, J. L. *J. Am. Chem. Soc.* **2005**, *127*, 12416−12422.
(6) Dawes, S. B.; Eglin, J. L.; Moeggenborg, K. J.; Kim, J.; Dye, J. L. *J. Am. Chem. Soc.* **1991**, *113*, 1605−1609. Wagner, M. J.; Huang, R. H.; Eglin, J. L.; Dye, J. L. *Nature* **1994**, *368*, 726−729.
(7) Huang, R. H.; Faber, M. K.; Moeggenborg, K. J.; Ward, D. L.; Dye, J. L. *Nature* **1998**, *331*, 599−601.
(8) Matsuishi, S.; Toda, Y.; Miyakawa, M.; Hayashi, K.; Kamiya, T.; Hirano, M.; Tanaka, I.; Hosono, H. *Science* **2003**, *301*, 626−629.
(9) Bartl, H.; Scheller, T. *Neues Jahrb. Mineral., Monatsh.* **1970**, *35*, 547−552.
(10) Jeevaratnam, J.; Glasser, F. P.; Glasser, L. S. D. *J. Am. Ceram. Soc.* **1964**, *47*, 105−106.
(11) Imlach, J. A.; Glasser, L. S. D.; Glasser, F. P. *Cem. Concr. Res.* **1971**, *1*, 57−61.
(12) Nurse, R. W.; Welch, J. H.; Majumdar, A. J. *Trans. Br. Ceram. Soc.* **1965**, *64*, 323−332.
(13) Hosono, H.; Abe, Y. *Inorg. Chem.* **1987**, *26*, 1192−1195.
(14) Li, Q.-X.; Hayashi, K.; Nishioka, M.; Kashiwagi, H.; Hirano, M.; Torimoto, Y.; Hosono, H.; Sadakata, M. *Appl. Phys. Lett.* **2002**, *80*, 4259−4261.
(15) Hayashi, K.; Hirano, M.; Matsuishi, S.; Hosono, H. *J. Am. Chem. Soc.* **2002**, *124*, 738−739.
(16) Hayashi, K.; Matsuishi, S.; Kamiya, T.; Hirano, M.; Hosono, H. *Nature* **2002**, *419*, 462−465.

10.1021/cm052367e CCC: $33.50 
Published on Web 03/09/2006

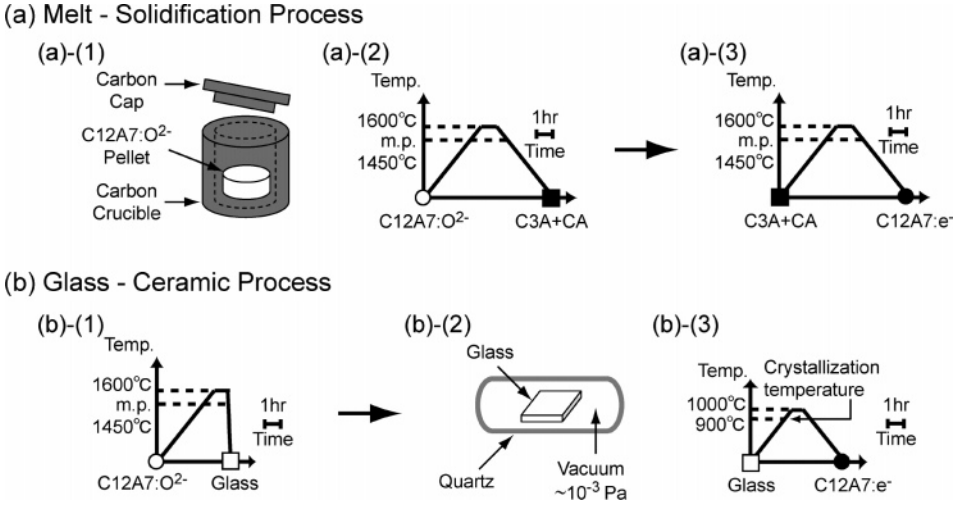


**Figure 1.** Schematic illustration of the synthesis processes for the C12A7 electride (C12A7:e$^-$) via the melt. (a) The solidification of C12A7:e$^-$ from the melt under a reducing atmosphere (melt-solidification process). The reducing atmosphere is achieved by heating a carbon crucible with a carbon cap at 1600 °C for 1 h ((a)−(1)). The first solidified product of C3A + CA is obtained according to the temperature profile shown in ((a)−(2)), but the second solidified product changes to a polycrystalline C12A7:e$^-$ (temperature profile: (a)−(3)). (b) The crystallization of transparent reduced glass under a vacuum (glass-ceramic process). The transparent reduced glass is obtained by quenching the melt according to the temperature profile shown in ((b)−(1)). The glass is encapsulated in a $SiO_2$ glass ampule under a vacuum and heated at 1000 °C for 30 min ((b)−(2)). The crystallized glass is a polycrystalline C12A7:e$^-$.

and leaves semilocalized electrons in the cages to form the electrical conductive C12A7. The electron concentration increases with the annealing time until the C12A7 with the theoretical maximum value of $2.33 \times 10^{21}$ cm$^{-3}$ is formed. The resulting $[Ca_{24}Al_{28}O_{64}]^{4+}(4e^-)$ may be regarded as a new type of electride, where electrons are not fully, but partially, localized in the cage, playing the role of anions, although it still remains controversial as to whether the electron-encaged C12A7 is an electride or not, based on the degree of the delocalization of the electrons.[17−20] Hereafter, C12A7 containing various amount of electrons, whose distinct electronic properties including the electron mobility and the work function for the electron emission are shown to be insensitive to the concentration, is referred to as the "C12A7 electride" or "C12A7:e$^-$" for simplicity.

The calcium vapor treatment process, which requires a single crystal[21] and a long annealing time (∼10 days),[8] is unsuitable for fabricating large-size C12A7:e$^-$ efficiently. In addition, the Ca treatment is not applicable to polycrystalline C12A7:e$^-$ synthesis. Thus, a simple synthetic method to fabricate C12A7:e$^-$ is necessary for various applications. Our strategy is focused on melt-solidification or glass-ceramics processing of C12A7 under a reducing atmosphere because only the reducing atmosphere has the potential to exclude the extraframework $O^{2-}$ ions during the solidification, simultaneously generating electrons in the cages. However, the process has a distinct drawback in that the reducing atmospheres hardly involve an anion that works as the template. It is known that the solidification from the melt with the 12CaO·7Al$_2$O$_3$ composition is markedly affected by the presence of template anions that promotes the precipitation of the crystalline C12A7 phase: the crystalline C12A7 phase is reproducibly prepared from a stoichiometric C12A7 melt in wet air,[9−13] involving $O^{2-}$ and/or $OH^-$ ions that act as the template. In contrast, the absence of template anions under a reducing atmosphere hinders the formation of the C12A7 phase and leads to the precipitation of the 3CaO·Al$_2$O$_3$ + CaO·Al$_2$O$_3$ (C3A + CA) eutectic.[9−12] Thus, a key issue to prepare the C12A7 phase under a reducing atmosphere is to find a new template anion in the melt that is compatible with the reducing atmosphere.

In this study, we report a simple and direct method to synthesize polycrystalline C12A7:e$^-$ from the C12A7 "melt" under a reducing atmosphere (melt-solidification process) and the crystallization of the reduced "glass" (glass-ceramic process).[22] It is demonstrated that the $C_2^{2-}$ anion acts as the template anion in the reducing atmosphere and is responsible for forming the C12A7:e$^-$. We also examine the performance of the polycrystalline C12A7:e$^-$ as an electron field emitter.

## Experimental Section

Insulating C12A7 powders were synthesized by a conventional solid-state reaction from a stoichiometric mixture of high-purity $CaCO_3$ and $\gamma$-$Al_2O_3$ at 1300 °C for 12 h in an ambient atmosphere. The C12A7 powders were melted in a semiairtight carbon crucible with a carbon cap at 1600 °C for 1 h in air. Heating the carbon crucible at 1600 °C produced a strongly reducing atmosphere ($pO_2 \approx 10^{-16}$ atm) inside the crucible. As schematically shown in Figure 1(a)-(2), the crucible in the melt-solidification process was slowly cooled at a rate of ∼400 °C/h. Then it was reheated according to the temperature program outlined in Figure 1(a)-(3). For the glass-ceramic process, the melt in the crucible was rapidly cooled to RT to form a transparent glass (Figure 1(b)-(1)). Then the glass was crystallized in an evacuated silica tube by heating to 1000 °C (Figure 1(b)-(2), (3)), which is higher than the glass-transition temperature (∼830 °C).[22]

(17) Sushko, P.; Schluger, K.; Hayashi, K.; Hirano, M.; Hosono, H. *Phys. Rev. Lett.* **2003**, *91*, 126401.
(18) Medvedeva, J. E.; Freeman, A. J.; Bertoni, M. I.; Mason, T. O. *Phys. Rev. Lett.* **2004**, *93*, 016408.
(19) Medvedeva, J. E.; Freeman, A. J. *Appl. Phys. Lett.* **2004**, *85*, 955−957.
(20) Li, Z.; Yang, J.; Hou, J. G.; Zhu, Q. *Angew. Chem., Int. Ed.* **2004**, *43*, 6479−6482.
(21) Watauchi, S.; Tanaka, I.; Hayashi, K.; Hirano, M.; Hosono, H. *J. Cryst. Growth* **2002**, *237−239*, 801−805.
(22) Rosenflanz, A.; Frey, M.; Endres, B.; Anderson, T.; Richards, E.; Schardt, C. *Nature* **2004**, *430*, 761−764.

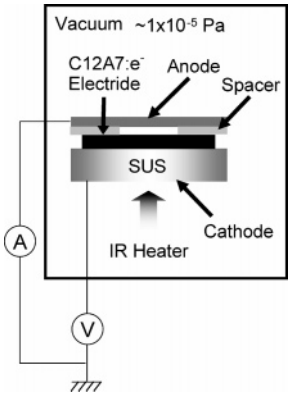


**Figure 2.** Schematic illustration of the setup for the electron field-emission measurements. A C12A7:$e^-$ plate is attached to a stainless steel plate (SUS) functioning as a cathode. A platinum film is deposited on the attached surface of the C12A7:$e^-$ plate to keep a good electrical contact with the SUS plate. The top surface is polished to a mirror surface using abrasive powders with a ~1 $\mu$m diameter. The separation between the cathode (the top surface of the C12A7:$e^-$ plate) and the anode made of copper plate is precisely adjusted to 0.05 mm using a 0.05 mm thick mica plate as a spacer.

The crystalline and glassy phases were identified by X-ray diffractometry (XRD) using a Rigaku RINT 2000. The microstructures were observed using an optical microscope. The solidified samples were crushed into fine powders, diluted with KBr powders, and subsequently pressed into pellets for optical diffuse reflectance measurements at RT. The Kubelka−Munk transformation was used to convert the measured spectra into absorption spectra. The electrical conductivity was measured using the four-probe method in a temperature range from RT to 20 K. The carrier electron concentration was determined by electron paramagnetic spin resonance (EPR) using a Bruker E580 X-band (~9.7 GHz) spectrometer at RT. To avoid the skin depth effect due to carrier electrons, the samples were crushed into fine powders (~1 $\mu$m in diameter). The spin concentration was estimated by comparing the second integral of the spectrum to the $CuSO_4 \cdot 5H_2O$ standard. The Raman spectra were measured at RT using a Fourier transformation spectrometer with a CW-Nd:YAG laser (1064 nm) as an excitation light source or with the second harmonics of a CW-Nd:YAG laser (532 nm). The electron field emission measurement was performed with the setup illustrated in Figure 2[2]. The polycrystalline C12A7:$e^-$, whose top surface was polished to a mirror surface, was mounted on the cathode. The distance between the top surface and the anode was adjusted to 0.05 mm. The emission current was measured by applying a negative voltage to the cathode up to −5 kV in the temperature range from RT to 500 °C.

## Results and Discussion

**1. C12A7 Electride Synthesis by Solidification of a Reduced Melt.** The solidified product of the first melt-solidification process was colored gray and it was the C3A + CA eutectic revealed by the XRD pattern shown in Figure 3(b)-(2), indicating that the crystalline C12A7 phase is hardly formed because the extraframework $O^{2-}$ ions in the cages are preferentially extracted due to the reducing atmosphere: the absence of the template anion leads to the decomposition of the C12A7 phase into the C3A + CA eutectic. However, the remelting and solidification of the C3A + CA eutectic in the same atmosphere (second melt-solidification process) unexpectedly resulted in the formation of the C12A7 single phase (Figure 3(b)-(3)), suggesting that an unknown template anion, which will be assigned as $C_2^{2-}$ ions later, was

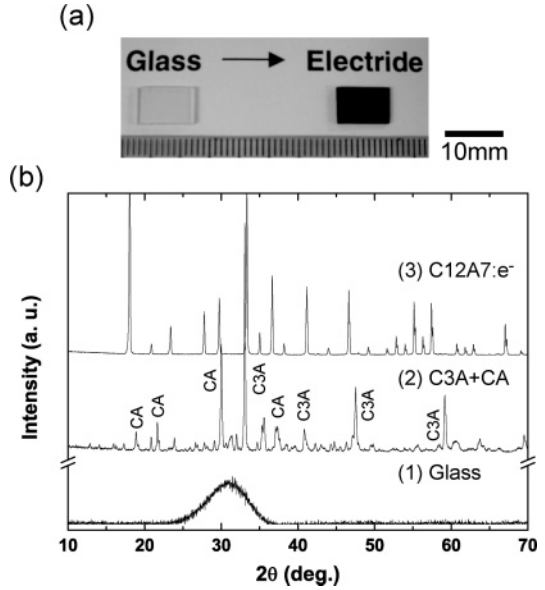


**Figure 3.** (a) Photograph of the reduced glass and the obtained C12A7 electride, showing the crystallization converts the transparent reduced glass into a dark green polycrystalline electride. (b) Powder X-ray diffraction patterns of (1) the transparent glass obtained by quenching the reduced melt, (2) the C3A + CA prepared by the first melt-solidification process, and (3) C12A7:$e^-$ by the second melt-solidification process. The pattern for the crystallized glass is the same as (3).

introduced in the melt during the second melt-solidification process. The obtained C12A7 was green in color and exhibited electrical conductivity, showing the incorporation of the electrons. The formation of the C12A7:$e^-$ in this two-step process is highly reproducible. In contrast, the formation of C12A7:$e^-$ by the one-step melt-solidification process scarcely occurred even under the optimized conditions estimated from Figure 8, such as keeping the melt at temperatures between 1415 and 1500 °C. These results suggest that the concentration of the unknown template anion in the melt is enhanced in the second process.

**2. C12A7 Electride Synthesis by Crystallization of a Reduced Glass.** First, a transparent glass was obtained by quenching the C12A7 melt in a carbon crucible with a carbon cap in air, which exhibited "photochromism": the glass turns gray in color upon exposure to ultraviolet (UV) radiation and is restored to its original color when the irradiation is terminated.[23] This property is commonly observed in C12A7 glass fabricated under the reducing conditions. Hence, the obtained glass is hereafter referred to as the "reduced glass". Differential thermal analysis revealed that the reduced glass is converted to crystalline C12A7 at the onset of the crystallization temperature ($T_c$), 900 °C. Then the reduced glass was encapsulated in a $SiO_2$ glass ampule under a vacuum and heated at 1000 °C for 30 min. The XRD diffraction pattern (Figure 3(b)-(3)) revealed that the precipitated phase was a single-crystalline C12A7. Moreover, it was dark green and electronically conductive (Figure 3(a)), which is similar to the precipitated C12A7 by the second melt-solidification process. The C12A7:$e^-$ prepared by the glass-ceramic process contained many cracks, presumably caused by the difference in the density between the reduced glass (2.92 g·cm$^{-3}$) and crystalline C12A7 (2.68 g·cm$^{-3}$).

(23) Hosono, H.; Asada, N.; Abe, Y. *J. Appl. Phys.* **1990**, *67*, 2840−2847.

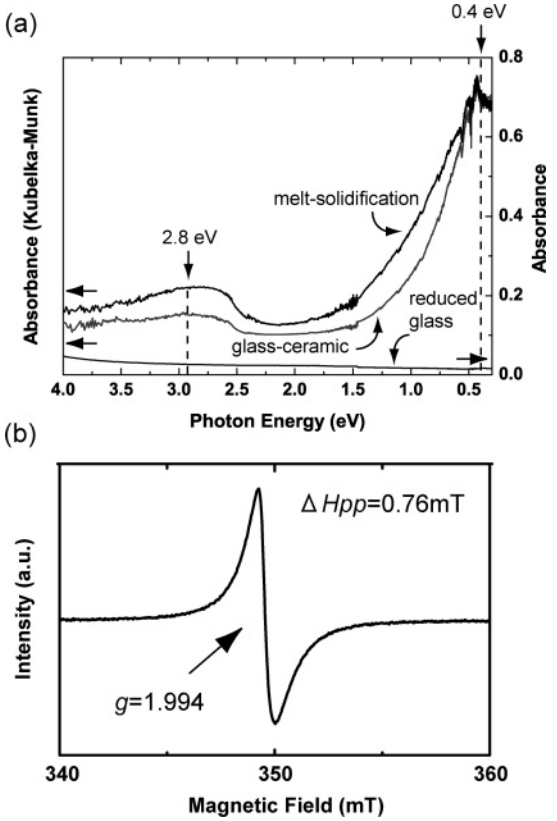


**Figure 4.** (a) Optical absorption spectra of the C12A7:e$^-$ prepared by the melt-solidification and glass-ceramic processes. The spectrum of the transparent reduced glass is also shown for comparison. Absorption spectra are obtained by converting diffuse reflectance spectra using Kubelka−Munk transformation. (b) X-band EPR spectrum of polycrystalline C12A7:e$^-$ with the electron concentration of ∼3 × 10$^{19}$ cm$^{-3}$ prepared by the melt-solidification process.

On the other hand, the C12A7 samples obtained from both the melt-solidification and glass-ceramic processes prepared in air using an alumina crucible, i.e., under an oxygen atmosphere, yielded electrically insulating white C12A7.

**3. Optical and EPR Spectra of Melt-Derived C12A7:e$^-$.** Figure 4(a) shows the optical absorption spectra of C12A7:e$^-$ prepared by the melt-solidification and glass-ceramic processes. That of the reduced glass is shown for comparison. Two distinct absorption bands at 0.4 and 2.8 eV are observed in the conductive samples. Ab initio calculations of the C12A7 electronic structure clarify that the two absorption bands are due to the intercage s-to-s transition and intracage s-to-p transition of the electrons trapped in the cages.[17,24]

Figure 4(b) is the EPR spectrum of C12A7:e$^-$ and shows an isotropic absorption band with $g = 1.994$. The observed spectrum is virtually identical to those of ultraviolet (UV) light-irradiated C12A7:H$^-$ [16] and the Ca-treated single-crystal C12A7:e$^-$.[8] The EPR band is assigned as associated with the electrons trapped in the cages. The concentration of electrons in the sample is evaluated as ∼3 × 10$^{19}$ cm$^{-3}$, which is the maximum value among C12A7:e$^-$ prepared in this study. The concentration could be enhanced up to the theoretical maximum value of 2.33 × 10$^{21}$ cm$^{-3}$ by optimizing process parameters such as $pO_2$ and/or modifying the process such as inclusion of additives in the melt.

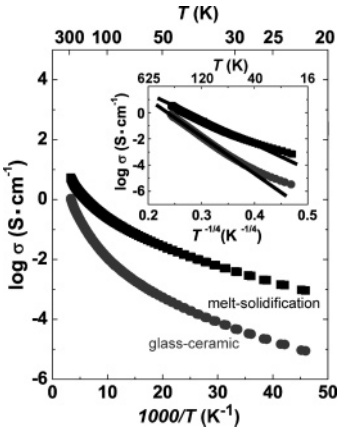


**Figure 5.** Temperature dependence of the electrical conductivity of polycrystalline C12A7:e$^-$ fabricated by the melt-solidification and glass-ceramic processes. Inset is the log $\sigma$ versus $T^{-1/4}$ plot.

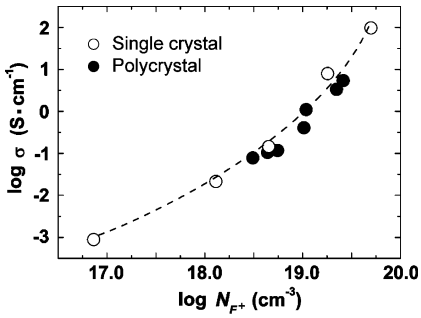


**Figure 6.** Electrical conductivity ($\sigma$) versus electron concentration ($N_{F+}$) for the polycrystalline and single-crystal electrides at 300 K. $N_{F+}$ is estimated from the optical absorption and EPR spectra. It indicates that the electron mobility of the polycrystalline C12A7:e$^-$ obtained via the melt is comparable to that of single-crystal C12A7:e$^-$ with the same electron concentration.

**4. Electrical Properties of Melt-Derived C12A7:e$^-$.** Figure 5 shows the temperature dependence of the electrical conductivity for the melt-derived polycrystalline C12A7:e$^-$. The conductivities at 300 K for the C12A7:e$^-$ by the melt-solidification and the glass-ceramic processes are 5 and 1 S·cm$^{-1}$, respectively. The conductivities exhibit a semiconducting nature, decreasing with temperature. The logarithm of the electrical conductivity is proportional to $T^{-1/4}$ and not $T^{-1}$ over a wide temperature range of 300−50 K (inset of Figure 5), suggesting the electron can be regarded as a "polaron". These characteristics are the same as those observed in the UV light-irradiated C12A7:H$^-$.[16]

Figure 6 shows the correlation between the electrical conductivity and the electron concentration estimated from the EPR spectra in the melt-derived polycrystalline C12A7:e$^-$ and the Ca-treated single-crystal C12A7:e$^-$. It is found that the two types of C12A7:e$^-$ exhibit similar electron mobilities, ∼0.1 cm$^2$·V$^{-1}$·s$^{-1}$.[8] Since the polycrystalline C12A7:e$^-$ are composed of coarse grains (∼3 mm) that are tightly connected, the influence of the grain boundaries on the electron mobility is likely negligibly small.

**5. Formation Mechanism for Electron.** Figure 7(a) shows the Raman spectra of C3A + CA and the transparent reduced glass. Bands that peak at ∼1870 cm$^{-1}$ are observed in both spectra, which are assigned to the $C_2^{2-}$ ion from a coincidence with spectrum of $CaC_2$ powder shown in Figure

(24) Sushko, P.; Schluger, K.; Hayashi, K.; Hirano, M.; Hosono, H. *Thin Solid Films* **2003**, *445*, 161−167.

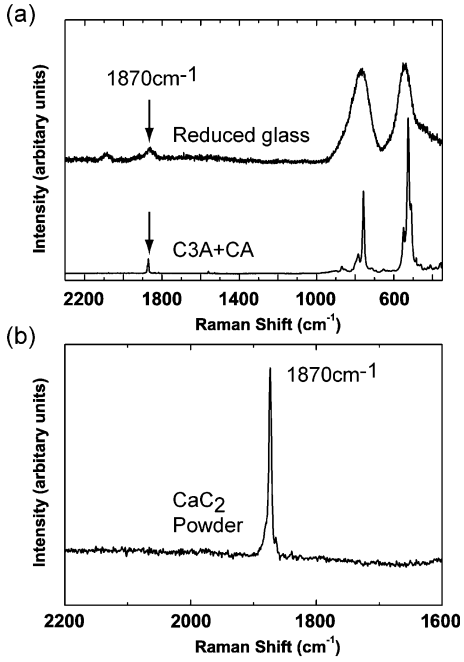


**Figure 7.** (a) Raman spectra of C3A + CA precipitated from the first melt-solidification process and the reduced glass. Arrows denote a 1870 $cm^{-1}$ band, which is assigned as associated with $C_2^{2-}$ ion based on an agreement in energy with the Raman band of $CaC_2$. (b) Raman spectrum of $CaC_2$ powder.

7(b). It is likely that the $C_2^{2-}$ ions are dissolved into the melt from the carbon crucible to compensate for the oxygen deficiency caused by the strongly reducing atmosphere. The ionic radius of $C_2^{2-}$ (1.2 Å) is similar to that of $O^{2-}$ (1.4 Å), which suggests that the $C_2^{2-}$ anions serve as the template in a reducing atmosphere, instead of the extraframework $O^{2-}$ ions in an oxidizing atmosphere.

The disappearance of the $C_2^{2-}$ Raman band after crystallization implies that the encaged $C_2^{2-}$ ions are only stable in the nucleation and/or initial stage of crystallization. Thermal desorption measurements reveal that CO gas is evolved from the C3A + CA around 800−1000 °C and from the crystallization process of the glass at ∼1000 °C. These observations further support that the encaged $C_2^{2-}$ ions are released from the cages, leaving electrons in the lattice. Thus, the total electron formation processes in the cages may be expressed by the following reactions:

$$C_2^{2-}\ (\text{melt or glass}) \rightarrow C_2^{2-}\ (\text{cage}) \rightarrow 2C\ (\text{solid}) + 2e^-\ (\text{cage}) \quad (1)$$

and/or

$$C_2^{2-}\ (\text{cage}) + 2O^{2-}\ (\text{cage}) \rightarrow 2CO\ (\text{atmosphere}) + 6e^-\ (\text{cage}) \quad (2)$$

Figure 8 illustrates the probable precipitated phase diagram of the $CaO-Al_2O_3$ system for the stoichiometric C12A7 melt in terms of temperature and atmosphere. When the melting temperature is higher than ∼1500 °C, the C12A7 phase tends to decompose into the C3A + CA under moisture-free, reducing, and inert gas atmospheres.[12] The C12A7 phase is obtained from a melt between 1415 and 1500 °C for 1 h under each atmosphere. However, if one keeps the melt for

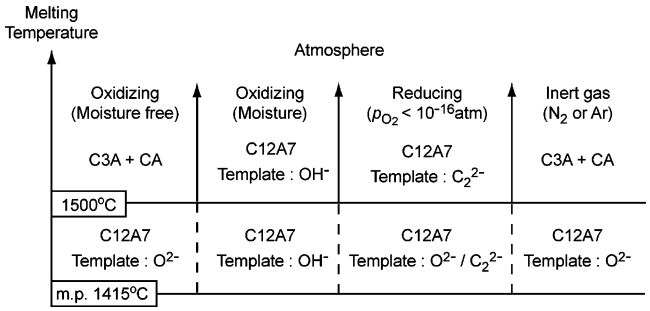


**Figure 8.** Precipitated phases from the $CaO-Al_2O_3$ melt system in terms of melting temperature and atmosphere with and without the template anion.

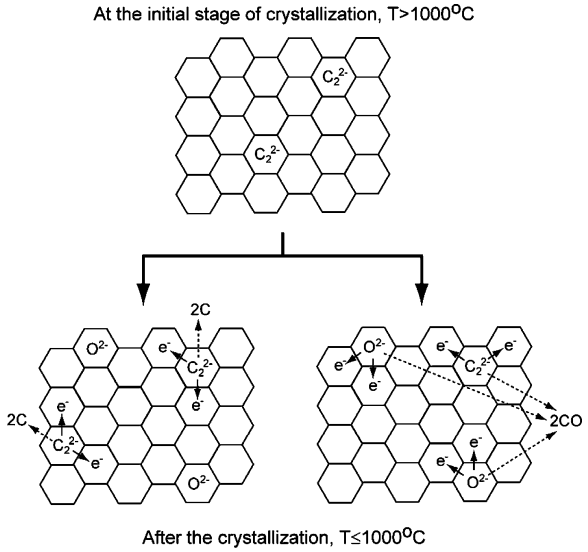


**Figure 9.** Model for the formation of electrons in the cages. The hexagon represents a crystallographic cage of C12A7. The top represents the nucleation and/or initial stage of the crystallization from the melt and the bottom shows the formation of electrons by releasing $C_2^{2-}$ during cooling.

a long time in the temperature range, $O^{2-}$ ions should be removed and the C12A7 phase will decompose into the C3A + CA mixture. Thus, the observation that the C12A7 phase was obtained as a final product under a strongly reducing atmosphere for melting temperatures higher than ∼1500 °C indicates that the $C_2^{2-}$ ion may act as the template at these higher temperatures just like the $OH^-$ ion.

Figure 9 illustrates the most likely mechanism for the electron formation in the cages, where the hexagon represents a crystallographic cage of C12A7. The cage structure is formed around the $C_2^{2-}$ anions at the nucleation and/or initial stage of crystallization and the C12A7 phase with the $C_2^{2-}$ anions trapped in the cages is developed (top chart in Figure 9). However, during the cooling process of C12A7:$C_2^{2-}$, the $C_2^{2-}$ ions are released from the cages in the form of either C or CO (bottom chart in Figure 9), leaving electrons in the lattice. The $C_2^{2-}$ ions play a similar role in the crystallization process of the reduced glass.

The present synthetic methods of the C12A7:$e^-$ are dependent on the heating, melting, and cooling procedures. Since the $C_2^{2-}$ ions are the origin of the trapped electrons, as postulated, the trapped $C_2^{2-}$ ions might be removed by leaving electrons during the cooling process. This indicates that the modification of process parameters such as the $pO_2$ and synthetic procedures such as the cooling process can vary the balance of the concentrations of trapped anions. It

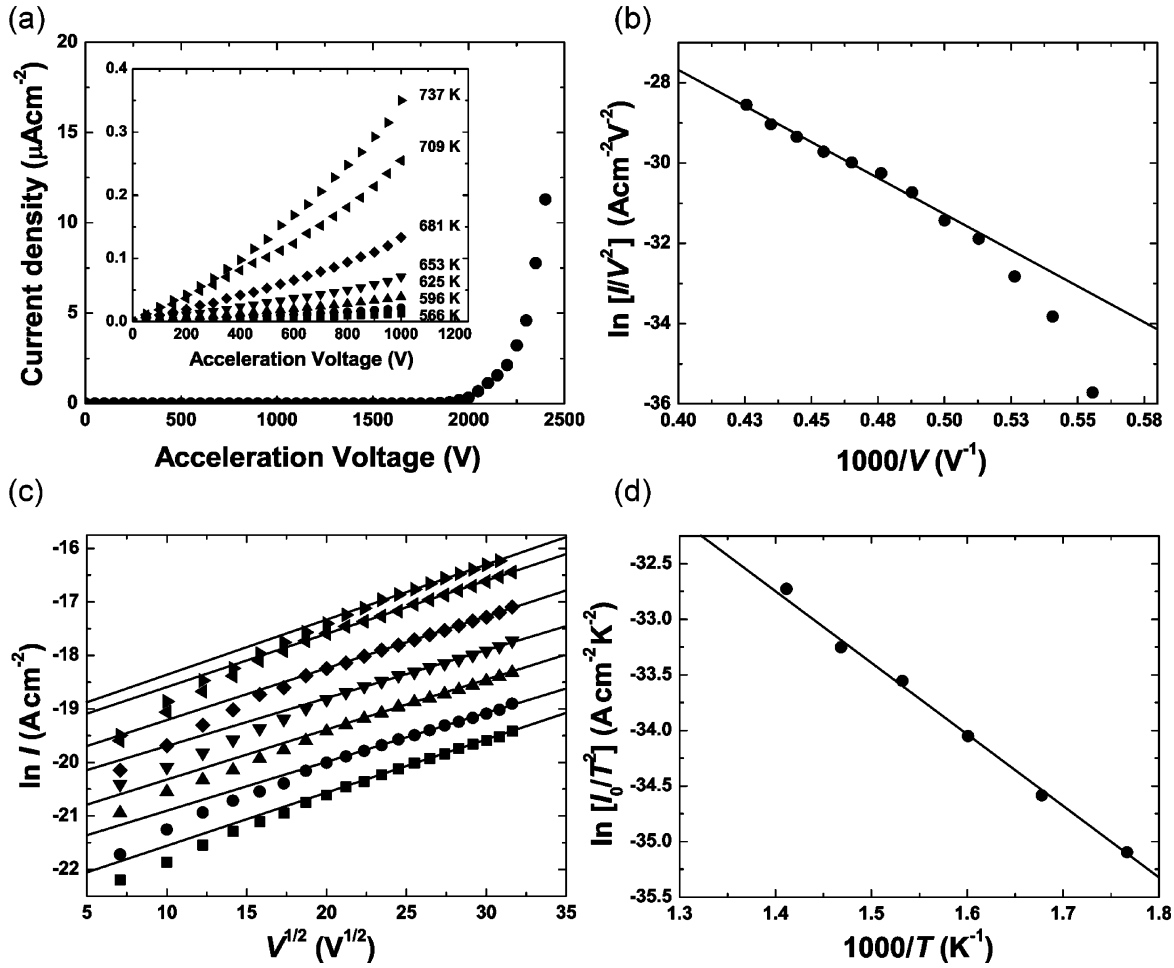


**Figure 10.** Characteristics of electron field emission for the polycrystalline C12A7:e$^-$. (a) $I-V$ characteristics for the electron emissionl (b) Fowler−Nordheim plot at room temperature; (c) Richardson−Dushman plot for the thermionic emission between 566 and 737 K; (d) $I_0/T^2$ versus $1/T$ plot. The work function estimated from the slope is ∼0.6 eV.

would be therefore worthwhile to further improve the present synthetic methods for the preparation of polycrystalline C12A7:e$^-$ with electron concentrations close to the stoichiometric values.

**6. Electron Emission Properties.** Figure 10(a) shows the emission current ($I$) as a function of applied voltage ($V$) at RT. The emission current starts to appear at ∼2 kV. The current density reaches 12 $\mu$A·cm$^{-2}$ at an electric field of 2.4 × 10$^5$ V·cm$^{-1}$. Figure 10(b) shows the $\ln(I/V^2) - 1/V$ plot of the experimental data (solid circles) in Figure 10(a). The solid line is derived from the Fowler−Nordheim tunneling model (F−N model) expressed by eq 3,

$$I = A\frac{(\beta V)^2}{\alpha\Phi}\exp\left(-\frac{B\Phi^{3/2}}{\beta V}\right) \tag{3}$$

where $A$ and $B$ are constants that are respectively estimated as 1.5 × 10$^{-6}$ (A·eV·V$^{-2}$) and 6.8 × 10$^{-7}$ (eV$^{-3/2}$·V·cm$^{-1}$). $\alpha$ is the emitting area, $\beta$ is the structure factor, and $\Phi$ is the work function. The good linearity except in the high voltage ranges as observed in Figure 10(b) indicates that the emission follows the F−N tunneling model. The inset of Figure 10(a) shows that the acceleration voltage is dependent on the emission currents for several temperatures. The current increases with temperature when the acceleration voltage is less than 1 kV. In this range, the emission property follows the field-assisted themionic emission model ($\ln I - V^{1/2}$ plot) as shown in Figure 10(c). The model is represented by eq 4,

$$I = I_0\exp\left(\frac{e}{kT}\sqrt{\frac{e\beta V}{4\pi\epsilon_0}}\right) \tag{4}$$

where $I_0$ is the prefactor, $k$ is the Boltzmann constant, and $\epsilon_0$ is the dielectric constant. These results indicate that the electron emission is dominated by the field-assisted thermionic emission at low extraction voltages, but as the acceleration voltage increases, the dominant emission mechanism changes to the Fowler−Nordheim tunneling. The work function ($\Phi$) is obtained from the Richardson−Dushman plot (R−D plot) expressed by eq 5,

$$I_0 = \frac{RT^2}{\alpha}\exp\left(-\frac{\Phi}{kT}\right) \tag{5}$$

where $R$ is a constant. Figure 10(d) shows a linear relationship between $\ln(I_0/T^2)$ and $1000/T$. The work function estimated from the slope is ∼0.6 eV, which is consistent with that of a single-crystal C12A7:e$^-$ despite the differences in the electron carrier concentration and sample texture.[2] Furthermore, the value is comparable to those of crown-ether and cryptand-based organic electrides,[3] although a much larger emission current is obtained in the C12A7:e$^-$ than in the organic electrides. On the other hand, the emission current

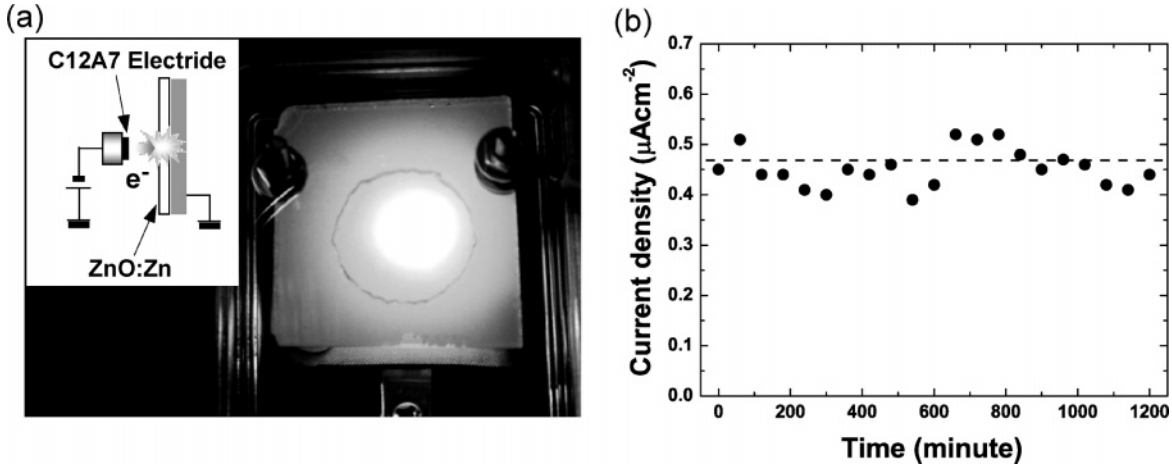


**Figure 11.** (a) Photograph of the field-emission light-emitting device at an extraction voltage of 3 kV. Inset schematically illustrates the triode-type device structure. (b) Variation of the emission current with time.

in the present study is much smaller than that obtained by a thermo-field emission (TFE) experiment at 900 °C (∼1.5 $A \cdot cm^{-2}$) using a single-crystal C12A7:$e^-$ subjected to a long aging at high temperature.[25] This is probably because the partial oxidation of the surface modifies the electron emission properties of the C12A7 electride. In other words, the work function for the emission current of C12A7:$e^-$ is improved by modifications of the surface.

We also demonstrated a field-emission display device where the polycrystalline C12A7:$e^-$ is used as an electron emitter and Zn-doped ZnO as a phosphor. As shown in Figure 11(a), the device, whose structure is illustrated in the inset, exhibits a bright emission at a 3 kV extraction voltage in typical ambient light. Furthermore, the emission current is stable over 1 day (Figure 11(b)), which implies that the C12A7:$e^-$ has potential as a cold-cathode electron emitter.

## Conclusions

A polycrystalline C12A7 electride is reproducibly fabricated by the solidification of the stoichiometric C12A7 melt under a reducing atmosphere and the crystallization of the reduced glass under a vacuum: via a melt-solidification process and a glass-ceramic process. The successful fabrication of a C12A7:$e^-$ under a reducing atmosphere is attributable to the existence of the carbon-related anion, $C_2^{2-}$, in the melt, which was kept in a semiairtight carbon crucible. The $C_2^{2-}$ ion serves as the template anion, instead of $O^{2-}$ anions, to stabilize the C12A7 phase. Further, it is removed from the lattice, leaving electrons in the cages during the crystallization processes. The resultant polycrystalline C12A7:$e^-$ shows an electrical conductivity up to ∼5 $S \cdot cm^{-1}$, which corresponds to a maximum electron concentration of $\sim 3 \times 10^{19}$ $cm^{-3}$. It is also noted that the polycrystalline C12A7:$e^-$ has nearly the same carrier mobility (∼0.1 $cm^2 \cdot V^{-1} \cdot s^{-1}$) as that of a single-crystal C12A7:$e^-$. The polycrystalline C12A7:$e^-$ yields a rather small work function of ∼0.6 eV for the electron emission, which has the potential for use in a cold-cathode electron-field emitter. The present methods are compatible with simple and efficient preparation of polycrystalline C12A7:$e^-$ and may cultivate various applications of the RT stable electride.

**Acknowledgment.** The authors thank Takashi Sakai for experimental assistance. This work is supported by a Grant-in-Aid for Creative Scientific Research (No. 16GS0205) from the Japanese Ministry of Education, Culture, Sports, Science and Technology.

CM052367E

(25) Toda, Y.; Kim, S. W.; Hayashi, K.; Hirano, M.; Kamiya, T.; Hosono, H.; Haraguchi, T.; Yasuda, H. *Appl. Phys. Lett.* **2005**, *87*, 254103.